



On a class of Bézier-like model for shape-preserving approximation

B. Nouri and J. Saeidian*

Abstract

A class of Bernstein-like basis functions, equipped with a shape parameter, is presented. Employing the introduced basis functions, the corresponding curve and surface in rectangular patches are defined based on some control points. It is verified that the new curve and surface have most properties of the classical Bézier curves and surfaces. The shape parameter helps to adjust the shape of the curve and surface while the control points are fixed. We prove that the proposed Bézier-like curves can preserve monotonicity and that Bézier-like surfaces can preserve axial monotonicity. Moreover, the presented curves and surfaces preserve bound constraints implied by the original data.

AMS subject classifications (2020): 65D17, 65D10, 68U05.

Keywords: Blending functions; Bézier curve; Shape adjustment; Monotonicity preservation; Shape-preserving; Boundedness.

1 Introduction

In computer-aided geometric design (CAGD) and computer graphics, curves are often constructed by the following relation:

* Corresponding author

Received 6 October 2022; revised 21 February 2022; accepted 12 March 2022

Bahareh Nouri

Faculty of Mathematical Sciences and Computer, Kharazmi University, Tehran, Iran.

e-mail: std_nouri411@khu.ac.ir

Jamshid Saeidian

Faculty of Mathematical Sciences and Computer, Kharazmi University, Tehran, Iran.

e-mail: j.saeidian@khu.ac.ir

$$C(t) = \sum_{i=0}^n F_i(t)P_i, \quad t \in [a, b] \subseteq \mathbb{R}, \quad n \in \mathbb{N}, \quad (1)$$

where the real functions $\{F_i\}$ are known as blending functions, $\{P_i\} \subseteq \mathbb{R}^s$ are control points ($s \geq 2$), and the polyline constructed by control points is called the control polygon. One of the most important blending functions are the Bernstein polynomials, which in turn lead to well-known classical Bézier curves. They have a simple structure and are widely used in many engineering and technology fields.

In a classical Bézier curve, once the control points are fixed, the shape of the curve cannot be changed. This is a drawback that reduces the shape adjustment and therefore limits their applicability. In order to overcome this deficiency, many researchers have tried to construct basis functions equipped with shape parameter(s) to create new curves whose structures and properties are similar to the Bézier curves, besides they also have the shape adjustment property [6, 13, 16, 17, 19, 21, 22, 23, 30]

In curves with shape parameter(s), by changing the parameter(s), the curve either approaches to the control polygon [17, 18, 19], or moves away from it [20, 31]. Another difference between parameter based curves originates from their construction, some basis functions are defined by a recursive formula [23, 22, 5, 20, 32], while others are based on a general formula [17, 19, 16, 18, 24, 8].

Here, we propose a new family of parameter based blending functions by using square roots of polynomials. Thus we call them *sq-basis functions*. The new blending functions are generated from three initial basis functions employing a recursive relation. This is a procedure that could be traced back in the literature [5, 22, 23, 32]. The corresponding Bézier-like curves, which in turn are referred to *sq-curves*, are in common with the classical Bézier curves in many features such as geometric invariance, endpoint interpolation, formal symmetry, and convex hull property. The sq-basis functions are equipped with one shape parameter, which can adjust the shape of the curve, and they would either move closer to or away from the control polygon. In the sq-curves with three control points, by altering the shape parameter, one would see a family of curves traveling from the control polygon to the straight line joining the first and last control point. In comparison to previously defined blending functions with the same structure, sq-curves show a higher rate of change by employing just one shape parameter, and this could be considered as an advantage. The construction could be extended to surfaces [11, 14], which share the most common features of Bézier surfaces.

Once we have a suitable model for data approximation, one can apply it in a shape-preserving approximation. Shape-preserving approximation is defined to be a method of constructing a curve (surface), which also preserves the shape implied by the data. It is known as an essential curve/surface design technique in CAD/CAM and geometric design. Convexity, monotonicity, positivity, and boundedness are the most important shape features,

which have extensively been studied in literature [1, 2, 3, 25, 27, 28, 29]. The proposed Bézier-like curves and surfaces prove to be a promising approximation tool that preserves the monotonicity and the boundedness implied by the data set.

The present paper is outlined as follows. In Section 2, the new blending functions are defined and their properties are studied. The corresponding curves and surfaces are defined in Section 3. Section 4 studies the shape-preserving properties of the new curves and surfaces.

2 New blending functions

The classical Bernstein functions have a number of important features that makes them a suitable basis for constructing control point based curves. Non-negativity, partition of unity, symmetry in some sense, and their end point values are among the most cited properties of classical Bernstein functions.

Here we address a general representation for a class of blending functions that have similar properties to Bernstein polynomials. We present a special case that uses the square root of quadratic (sq) polynomials.

Definition 1. Based on a real valued shape parameter ν , the sq-starting basis functions are defined as follows:

$$\begin{aligned} b_{2,0}(t) &= \frac{1}{2} - t + \varphi(t), \\ b_{2,1}(t) &= 1 - 2\varphi(t), \\ b_{2,2}(t) &= t - \frac{1}{2} + \varphi(t), \end{aligned} \quad (2)$$

where $0 \leq t \leq 1$, $0 < \nu \leq 1$, and

$$\varphi(t) = \sqrt{(1 - \nu)(t^2 - t) + \frac{1}{4}}.$$

We generate the sq-basis functions of order n ($n \geq 3$) with the recursion relation of the classical Bernstein basis functions [9] as follows:

$$b_{n,i}(t) = (1 - t)b_{n-1,i}(t) + tb_{n-1,i-1}(t), \quad t \in [0, 1], \quad (3)$$

where $i = 0, 1, 2, \dots, n$. For $k = -1$ or $k > n$, we set $b_{n,k}(t) = 0$.

The sq-basis functions of order $n = 3$ can be expressed as

$$\begin{aligned} b_{3,0}(t) &= t^2 - \frac{3}{2}t + \frac{1}{2} + (1 - t)\varphi(t), \\ b_{3,1}(t) &= -t^2 - \frac{1}{2}t + 1 + (-2 + 3t)\varphi(t), \end{aligned} \quad (4)$$

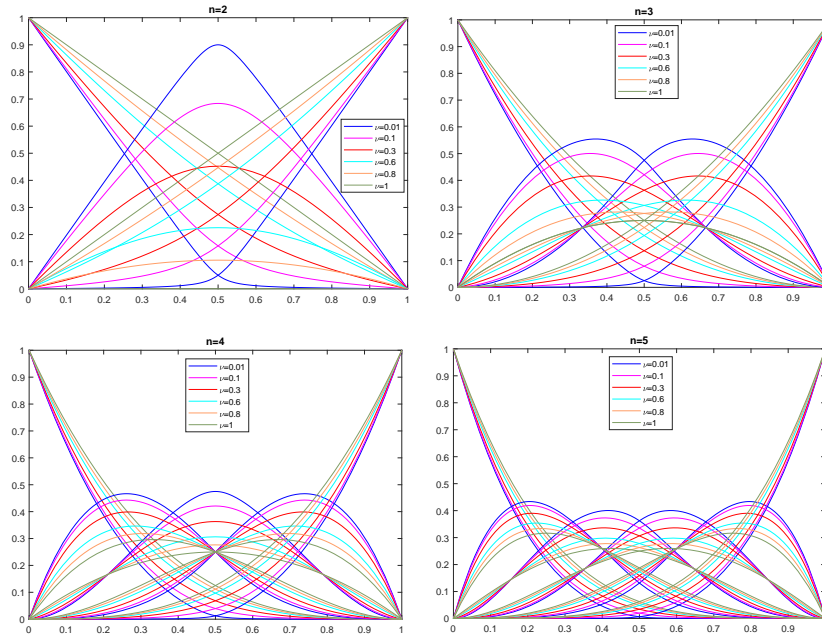


Figure 1: The sq-basis functions with different values of ν .

$$b_{3,2}(t) = -t^2 + \frac{5}{2}t - \frac{1}{2} + (1 - 3t)\varphi(t),$$

$$b_{3,3}(t) = t^2 - \frac{1}{2}t + t\varphi(t).$$

Figure 1 shows the sq-basis functions generated with $n = 2, 3, 4, 5$ and different values of ν .

Theorem 1. The sq-basis functions generated by (2) and (3) have the following properties:

- (a) Nonnegativity: $b_{n,i}(t) \geq 0$ for $i = 0, 1, 2, \dots, n$.
- (b) Partition of unity (Normalization): $\sum_{i=0}^n b_{n,i}(t) = 1$.
- (c) Symmetry: $b_{n,i}(t) = b_{n,n-i}(1 - t)$ for $i = 0, 1, 2, \dots, n$.
- (d) End-point values:

$$b_{n,i}(0) = \begin{cases} 1, & i = 0, \\ 0, & i \neq 0, \end{cases} \quad b_{n,i}(1) = \begin{cases} 1, & i = n, \\ 0, & i \neq n, \end{cases} \quad (5)$$

$$b'_{n,i}(0) = \begin{cases} -n + \nu, & i = 0, \\ n - 2\nu, & i = 1, \\ \nu, & i = 2, \\ 0, & o.w., \end{cases} \quad b'_{n,i}(1) = \begin{cases} n - \nu, & i = n, \\ 2\nu - n, & i = n - 1, \\ -\nu, & i = n - 2, \\ 0, & o.w. \end{cases} \quad (6)$$

Proof. Mathematical induction is used to prove this theorem.

- (a) Nonnegativity is obvious from (2) and (3).
- (b) From (2), we obtain $\sum_{i=0}^2 b_{2,i}(t) = 1$. Now suppose that the equality is true for m . Then according to recurrence relation(3) and the inductive hypothesis, we obtain

$$\sum_{i=0}^{m+1} b_{m+1,i}(t) = (1-t) \sum_{i=0}^{m+1} b_{m,i}(t) + t \sum_{i=0}^{m+1} b_{m,i-1}(t) = 1 - t + t = 1.$$

- (c) The sq-starting basis functions are symmetrical. Assume that the sq-basis functions of order m are symmetrical. Then from this inductive hypothesis and recurrence relation (3), one has

$$\begin{aligned} b_{m+1,i}(1-t) &= (1 - (1-t))b_{m,i}(1-t) + (1-t)b_{m,i-1}(1-t) \\ &= tb_{m,m-i}(t) + (1-t)b_{m,m-i+1}(t) = b_{m+1,m-i+1}(t). \end{aligned}$$

- (d) From (2), we have

$$\begin{aligned} b'_{2,0}(t) &= -1 + \varphi'(t), \\ b'_{2,1}(t) &= -2\varphi'(t), \\ b'_{2,2}(t) &= 1 + \varphi'(t), \end{aligned} \quad (7)$$

where

$$\varphi'(t) = \frac{(1-\nu)(2t-1)}{2\sqrt{(1-\nu)(t^2-t) + \frac{1}{4}}}.$$

By a simple deduction from (2) and (7), we conclude that the results in (5) and (6) hold for $n = 2$.

Suppose that the properties at the endpoints hold for the sq-basis functions of order m . Then

$$\begin{aligned} b_{m+1,i}(0) = b_{m,i}(0) &= \begin{cases} 1 & i = 0, \\ 0, & i \neq 0, \end{cases} \\ b_{m+1,i}(1) = b_{m,i}(1) &= \begin{cases} 1 & i = m, \\ 0, & i \neq m, \end{cases} \end{aligned} \quad (8)$$

which can be obtained by the inductive hypothesis and (3).

From (3), we have

$$b'_{m+1,i}(0) = -b_{m,i}(0) + b'_{m,i}(0) + b_{m,i-1}(0), \quad (9)$$

$$b'_{m+1,i}(1) = -b_{m,i}(1) + b_{m,i-1}(1) + b'_{m,i-1}(1). \quad (10)$$

From (8) and the inductive hypothesis and by using relation (9), the following results are obtained:

- (i) For $i = 0$, $b'_{m+1,0}(0) = -b_{m,0}(0) + b'_{m,0}(0) = -1 - (-m + \nu) = -(m + 1) + \nu$,
- (ii) For $i = 1$, $b'_{m+1,1}(0) = -b_{m,1}(0) + b'_{m,1}(0) + b_{m,0}(0) = (m + 1) - 2\nu$,
- (iii) For $i = 2$, $b'_{m+1,2}(0) = -b_{m,2}(0) + b'_{m,2}(0) + b_{m,1}(0) = 0 + \nu + 0 = \nu$,
- (iv) For $i \neq 0, 1, 2$, $b'_{m+1,i}(0) = 0$.

Similarly, from (10), the following results are deduced:

- (i) For $i = m + 1$, $b'_{m+1,m+1}(1) = (m + 1) - \nu$,
- (ii) For $i = m$, $b'_{m+1,m}(1) = -(m + 1) + 2\nu$,
- (iii) For $i = m - 1$, $b'_{m+1,m-1}(1) = -\nu$,
- (iv) For $i \neq m - 1, m, m + 1$, $b'_{m+1,i}(1) = 0$.

□

3 sq-curves and sq-surfaces

The sq-basis functions can be considered as blending functions to construct Bézier-like curves. Here we present the sq-curves and also extend the idea to surfaces.

Definition 2. Given control points $\{P_i\}_{i=0}^n \subseteq \mathbb{R}^2$, for $0 \leq t \leq 1$, $0 < \nu \leq 1$,

$$r_n(t) = \sum_{i=0}^n b_{n,i}(t)P_i, \quad (11)$$

is called a sq-curve, where $\{b_{n,i}(t)\}_{i=0}^n$ ($n \geq 3$) are the sq-basis functions defined in (2) and (3).

From Theorem 1, the sq-curve introduced in (11) has the following properties:

- (a) Geometric property at the endpoints: From the properties at the endpoints of the sq-basis functions, we obtain

$$\begin{aligned} r_n(0) &= P_0, & r_n(1) &= P_n, \\ r'_n(0) &= (\nu)(P_2 - 2P_1 + P_0) + n(P_1 - P_0), \\ r'_n(1) &= (-\nu)(P_n - 2P_{n-1} + P_{n-2}) + n(P_n - P_{n-1}). \end{aligned}$$

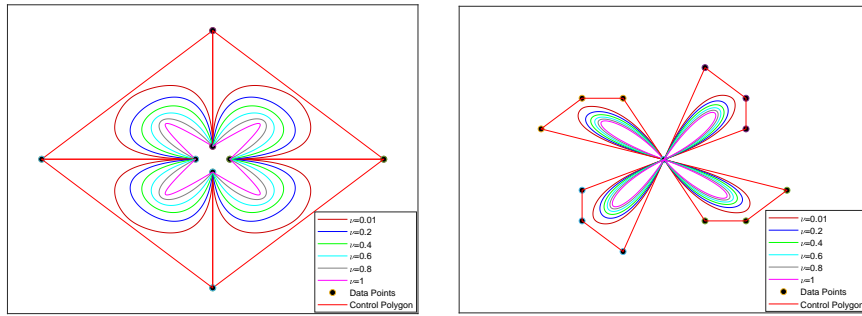


Figure 2: sq-curve with different values of ν .

- (b) Symmetry: The symmetry property of the sq-basis functions leads us to

$$\begin{aligned}
 r_n(t; P_0, P_1, \dots, P_n) &= \sum_{i=0}^n b_{n,i}(t)P_i = \sum_{i=0}^n b_{n,n-i}(1-t)P_i \\
 &= \sum_{j=0}^n b_{n,j}(1-t)P_{n-j} = r_n(1-t; P_n, P_{n-1}, \dots, P_0).
 \end{aligned}$$

- (c) Geometric invariance: As $r_n(t)$ is an affine combination of the control points, so the shape of the sq-curve is independent of the choice of coordinate system.
- (d) Convex hull property: Because of the nonnegativity and normalization properties of the sq-basis functions, one concludes that the sq-curve must be inside the convex hull of its control polygon.

Figure 2 shows two specific curves generated by sq-curves, in which the control points are fixed and values of ν are set to $\nu = 0.01, 0.2, 0.4, 0.6, 0.8, 1$, respectively, from outside to inside. One can see that the sq-curves are to approach the control polygon as the shape parameter decreases.

3.1 Comparison with existing basis functions

The construction of a suitable set of blending function has attracted a great deal of interest among scientists. The main goal of most papers in this filed is to construct parameter based blending functions, which by altering this parameter(s), one can make most changes in the corresponding parametric curve (1). Some works focus on a specific application, and others studied

the structure and construction strategies. Here, we aim to emphasize on advantages of the sq-basis functions. As the sq-basis functions are generated recursively, we compare them with those who have a recursion formula.

Figure 3 represents a visual comparison. Figure 3(a) shows the sq-curves; Figure 3(b) represents the curves constructed in [32]; and the curves proposed in [23] are depicted in Figures 3(c) and 3(d), for different values of shape parameters. Compared to [32], the rate of change in sq-curves is greater than changing the corresponding shape parameter. The curves generated in [23] show a good rate of change for different values of shape parameters, but this is achieved by employing two separate parameters. In the sq-curves, this much of flexibility is gained by altering just one shape parameter.

In [20], no curve can be constructed for three control points because the starting basis functions have four members. Authors in [5, 6, 22, 23] employed three starting basis functions, but several shape parameters were used to make further changes to the curves. However, in the case of sq-curves, the same changes are gained with just one parameter. In some works [31, 15, 4], only four [15, 4] or five [31] bases were presented, and curves with fewer control points cannot be represented by these basis functions. For more control points, the continuity conditions are checked.

Generally, among the Bézier-like curves, which aim to present curves that move from the convex combination of the first and last control points to the control polygon by altering shape parameter, the sq-curves serve as a good choice and compete well with the other bases.

3.2 sq-surface

The corresponding sq-surfaces can be constructed by a tensor product approach. Given control points $\{P_i\}_{i=0}^n \subseteq \mathbb{R}^3$, the surface represented by

$$S(s, t) = \sum_{i=0}^m \sum_{j=0}^n P_{i,j} b_{m,i}(s) b_{n,j}(t), \quad 0 \leq s, t \leq 1, \quad (12)$$

is called a sq-surface, in which $b_{m,i}(s)$ and $b_{n,j}(t)$ are the sq-basis functions.

Figure 4 shows that different surfaces can be obtained by altering the shape parameter when the control net is fixed.

From the properties of the sq-basis functions, it is easy to verify the following properties of the corresponding sq-surfaces:

- (a) Interpolation at the corner points: $S(s, t)$ passes through corner points $P_{0,0}, P_{m,0}, P_{0,n}$, and $P_{m,n}$. In fact, we have $S(0, 0) = P_{0,0}$, $S(1, 0) = P_{m,0}$, $S(0, 1) = P_{0,n}$, and $S(1, 1) = P_{m,n}$.
- (b) Nonnegativity: It is obvious that $b_{m,i}(s) b_{n,j}(t)$ is nonnegative for all m, n, i, j and $s, t \in [0, 1]$.

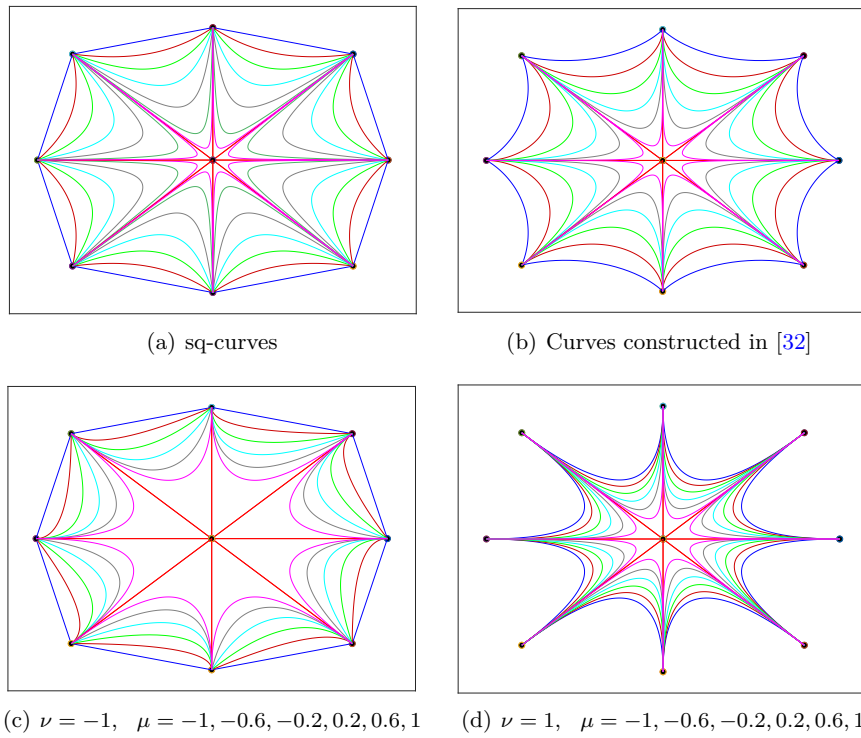


Figure 3: Comparison of sq-curves with curves proposed in [32] and [23]

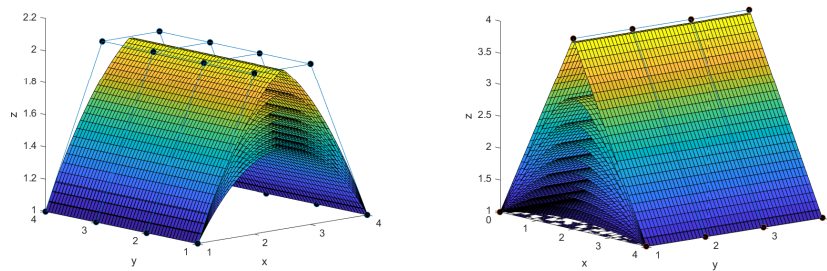


Figure 4: Shape of sq-surfaces with different shape parameters.

(c) Partition of unity:

$$\sum_{i=0}^m \sum_{j=0}^n b_{m,i}(s) b_{n,j}(t) = \sum_{i=0}^m b_{m,i}(s) \sum_{j=0}^n b_{n,j}(t) = 1, \quad 0 \leq s, t \leq 1.$$

Proof of this is due to the partition of unity of the sq-basis functions.

(d) Convex hull property: The surface lies in the convex hull of its control points, since $S(s, t)$ is the linear combination of its control points with positive coefficients that sums to 1 (partition of unity).

(e) Affine invariance: This means that the surface defined by control points that are an affine transformation of all control points is the same surface that is obtained by applying the same transformation to the surface's equation. As $S(s, t)$ is an affine combination of the control points, so the shape of the sq-surfaces is independent of the choice of coordinate system.

(f) Boundaries of surface: The four surface boundaries are exactly the four sq-curves defined by the boundary edges of the surface as follows:

$$\begin{aligned} S(0, t) &= \sum_{j=0}^n P_{0,j} b_{n,j}(t), & S(1, t) &= \sum_{j=0}^n P_{m,j} b_{n,j}(t), \\ S(s, 1) &= \sum_{i=0}^m P_{i,n} b_{m,i}(s), & S(s, 0) &= \sum_{i=0}^m P_{i,0} b_{m,i}(s). \end{aligned}$$

4 Shape-preserving approximation by sq-curves and sq-surfaces

The sq-curves preserve monotonicity and the sq-surfaces are axially monotonicity preserving. The newly defined models preserve boundedness in both two-dimensional and three-dimensional data. Here we state these facts in a detailed discussion.

4.1 Monotonicity preservation of sq-curves

Here, we present a proof of the monotonicity preservation of the sq-basis functions and sq-curves.

Definition 3. A system of functions (g_0, \dots, g_n) is monotonicity preserving if for any $\lambda_0 \leq \lambda_1 \leq \dots \leq \lambda_n$ in \mathbb{R} , the function $\sum_{i=0}^n \lambda_i g_i$ is increasing.

The following result, which characterizes monotonicity preserving systems, appears in [7, Proposition 2.3].

Proposition 1. Let (g_0, \dots, g_n) be a system of functions defined on an interval $[a, b]$. Let $v_i := \sum_{j=i}^n g_j$ for $i \in \{0, 1, \dots, n\}$. Then (g_0, \dots, g_n) is monotonicity preserving if and only if v_0 is a constant function and the functions v_i are increasing for $i = 1, \dots, n$.

We obtain the following result using the previous proposition.

Proposition 2. The sq-basis functions $(b_{n,0}, b_{n,1}, \dots, b_{n,n})$ defined by (2) and (3) are monotonicity preserving.

Proof. Let us consider sq-basis functions (2) with $n = 2$. Using Proposition 1, $(b_{2,0}, b_{2,1}, b_{2,2})$ is monotonicity preserving if v_0 is a constant function and the functions v_1 and v_2 are increasing. Moreover,

$$v_0 = \sum_{j=0}^2 b_{2,j}(t) = 1$$

and

$$v_1 = \sum_{j=1}^2 b_{2,j}(t) = b_{2,1}(t) + b_{2,2}(t) = \frac{1}{2} + t - \varphi(t) \Rightarrow v_1'(t) = 1 - \varphi'(t).$$

The function $\varphi(t)$ is a convex function in the interval $[0, 1]$, so the decreasing function $-\varphi'(t)$ takes its minimum at $t = 1$. Thus we have $v_1'(1) = \nu$, so $v_1'(t) \geq 0$ for all $t \in [0, 1]$. Therefore the function $v_1(t)$ is increasing. We have

$$v_2 = \sum_{j=2}^2 b_{2,j}(t) = b_{2,2}(t) = t - \frac{1}{2} + \varphi(t) \Rightarrow v_2'(t) = 1 + \varphi'(t).$$

Again, employing the convexity of $\varphi(t)$, one observes that the increasing function $\varphi'(t)$ takes its minimum at $t = 0$. Since $v_2'(0) = \nu$ results in $v_2'(t) \geq 0$, for all $t \in [0, 1]$, so we can conclude that $v_2(t)$ is an increasing function.

Suppose that the sq-basis functions $(b_{n-1,0}, b_{n-1,1}, \dots, b_{n-1,n-1})$ is monotonicity preserving. Then using Proposition 1, $(b_{n,0}, b_{n,1}, \dots, b_{n,n})$ is monotonicity preserving if v_0 is a constant function and the functions v_i are increasing for $i = 1, \dots, n$.

We have

$$v_0 = \sum_{j=0}^n b_{n,j}(t) = 1$$

and

$$v_i = \sum_{j=i}^n b_{n,j}(t) \Rightarrow v_i'(t) = \sum_{j=i}^n b'_{n,j}(t). \tag{13}$$

By combining formulas (3) and (13), we have

$$\begin{aligned}
 v'_i(t) &= -\sum_{j=i}^n b_{n-1,j}(t) + (1-t) \sum_{j=i}^n b'_{n-1,j}(t) + \sum_{j=i}^n b_{n-1,j-1}(t) + t \sum_{j=i}^n b'_{n-1,j-1}(t) \\
 &= b_{n-1,n} + \left(-\sum_{j=i}^{n-1} b_{n-1,j}(t) + \sum_{j=i}^{n-1} b_{n-1,j}(t) \right) + b_{n-1,i-1}(t) \\
 &\quad + (1-t) \sum_{j=i}^n b'_{n-1,j}(t) + t \sum_{j=i}^n b'_{n-1,j-1}(t) \\
 &= b_{n-1,i-1}(t) + (1-t) \sum_{j=i}^{n-1} b'_{n-1,j}(t) + t \sum_{j=i-1}^{n-1} b'_{n-1,j}(t). \tag{14}
 \end{aligned}$$

Since $(b_{n-1,0}, b_{n-1,1}, \dots, b_{n-1,n-1})$ is monotonicity preserving, we deduce

$$\sum_{j=i}^{n-1} b'_{n-1,j}(t) \geq 0, \quad \sum_{j=i-1}^{n-1} b'_{n-1,j}(t) \geq 0. \tag{15}$$

Now, from (14) and (15), for $t \in [0, 1]$, it is obvious that $v'_i(t) \geq 0$. \square

The sq-curve is a curve in \mathbb{R}^2 plane, so we need the following statement to assure the monotonicity preservation of sq-curves. The proof is straightforward.

Proposition 3. Let (g_0, \dots, g_n) be a system of functions that is monotonicity preserving. If $\{P_i\}_{i=0}^n \subseteq \mathbb{R}^2$ is the monotone data, then the function $\sum_{i=0}^n P_i g_i$ is increasing.

4.2 Monotonicity preservation of sq-surfaces

The sq-surfaces (12), defined on rectangular patches, are axially monotonicity-preserving. To verify this assertion, we state our reasoning based on some known results from the literature.

Given two strictly increasing sequences of abscissas $\alpha = (\alpha_0, \alpha_1, \dots, \alpha_m)$ and $\beta = (\beta_0, \beta_1, \dots, \beta_n)$ and control points $\left\{ \begin{pmatrix} \alpha_i \\ \beta_j \\ c_{ij} \end{pmatrix} \right\}_{i=0, \dots, m}^{j=0, \dots, n}$, we define the control net $p : [\alpha_0, \alpha_m] \times [\beta_0, \beta_n] \rightarrow \mathbb{R}$ to be the unique function that satisfies the interpolation conditions $p(\alpha_j, \beta_j) = c_{ij}$, for all $i = 0, 1, \dots, m$, and $j = 0, 1, \dots, n$, and is bilinear on each rectangle $R_{ij} = [\alpha_i, \alpha_{i+1}] \times [\beta_j, \beta_{j+1}]$.

A bivariate function g is increasing in a direction $d = (d_1, d_2) \in \mathbb{R}^2$, if $g(x + \lambda d_1, y + \lambda d_2) \geq g(x, y)$, $\lambda > 0$. In particular, the control net p can be

increasing in a direction d . This case has been characterized by Floater and Peña [10] in the following way.

Lemma 1. The control net p is increasing in the direction $d = (d_1, d_2) \in \mathbb{R}^2$ if and only if for $i = 0, 1, \dots, m - 1$ and $j = 0, 1, \dots, n - 1$,

$$d_1 \Delta_1 c_{i,j+l} + d_2 \Delta_2 c_{i+k,j} \geq 0, \quad k, l \in \{0, 1\},$$

where $\Delta_1 c_{ij} := (c_{i+1,j} - c_{i,j}) / (\alpha_{i+1} - \alpha_i)$ and $\Delta_2 c_{ij} := (c_{i,j+1} - c_{i,j}) / (\beta_{j+1} - \beta_j)$.

Given a sequence $(c_{ij})_{\substack{0 \leq j \leq n \\ 0 \leq i \leq m}}$, we have $\Lambda_1 c_{ij} : c_{i+1,j} - c_{i,j}$ for $i = 0, 1, \dots, m - 1$ and $j = 0, 1, \dots, n - 1$ and $\Lambda_2 c_{ij} : c_{i,j+1} - c_{i,j}$ for $i = 0, 1, \dots, m - 1$ and $j = 0, 1, \dots, n - 1$.

Remark 1. As a consequence of Lemma 1, we have that the control net p is increasing in the X -axis direction $d = (1, 0)$ if and only if for $i = 0, 1, \dots, m - 1$ and $j = 0, 1, \dots, n - 1$, $\Lambda_1 c_{ij} \geq 0$. Analogously, the control net p is increasing in the Y -axis direction $d = (0, 1)$ if and only if for $i = 0, 1, \dots, m - 1$ and $j = 0, 1, \dots, n - 1$, $\Lambda_2 c_{ij} \geq 0$.

Theorem 2. If the control net p is increasing in the X -axis direction $d = (1, 0)$ or in the Y -axis direction $d = (0, 1)$, then so is sq-surface $S(s, t)$.

Proof. Suppose that the control net p is increasing in the X -axis direction $d = (1, 0)$. Then for $i = 0, 1, \dots, m - 1$ and $j = 0, 1, \dots, n - 1$, we have $\Lambda_1 c_{ij} \geq 0$. We show that, in this case, $S(s, t)$ is increasing in the direction $d = (1, 0)$. Therefore,

$$S(s, t) = \sum_{i=0}^m \sum_{j=0}^n \begin{pmatrix} \alpha_i \\ \beta_j \\ c_{ij} \end{pmatrix} b_{m,i}(s) b_{n,j}(t), \quad 0 \leq s, t \leq 1.$$

The surface $S(s, t)$ in the direction $d = (1, 0)$ for specified $y = \gamma$ is a curve that is obtained from the collision of the plane $y = \gamma$ and the surface $S(s, t)$, so

$$\begin{aligned} \sum_{i=0}^m \sum_{j=0}^n \beta_j b_{m,i}(s) b_{n,j}(t) = \gamma &\Rightarrow \sum_{i=0}^m b_{m,i}(s) \sum_{j=0}^n \beta_j b_{n,j}(t) = \gamma \\ &\Rightarrow \sum_{j=0}^n \beta_j b_{n,j}(t) = \gamma. \end{aligned}$$

Therefore t is fixed and the curve on plane $y = \gamma$ is as follows:

$$\sum_{j=0}^n b_{n,j}(t) \left[\sum_{i=0}^m \begin{pmatrix} \alpha_i \\ c_{ij} \end{pmatrix} b_{m,i}(s) \right], \quad 0 \leq s \leq 1. \tag{16}$$

Now from Proposition 3, one observes that $\sum_{i=0}^m \binom{\alpha_i}{c_{ij}} b_{m,i}(s)$ is increasing for any j , which lead us to the conclusion that the curve (16) would be increasing. Because the value of γ was arbitrary, the surface $S(s, t)$ is increasing in the direction $d = (1, 0)$. One can prove the desired result in the direction $d = (0, 1)$, in a similar way. \square

Example 1. The set of data presented in Table 1 is generated from the function

$$F(x, y) = \ln(x^2 + y^2). \quad (17)$$

We have $\left\{ \binom{x_i}{y_j} \right\}_{i=0, \dots, 6}^{j=0, \dots, 6}$ as a data set in a three-dimensional space. These provide us 49 control points. By these control points, we have a control net p , which is increasing in the X -axis direction $d = (1, 0)$ and in the Y -axis direction $d = (0, 1)$. Figure 5 is the visual model of monotone surfaces in the X -axis direction and in the Y -axis direction that are obtained by control points and (12) with different values of free parameter ν . The error rate of monotone surfaces has been reported.

Table 1: Data generated from the function $F(x, y) = \ln(x^2 + y^2)$

y	x						
	20	40	60	80	100	200	300
20	6.6846	7.6009	8.2940	8.8247	9.2496	10.6066	11.4120
40	7.6009	8.0709	8.5564	8.9872	9.3588	10.6359	11.4252
60	8.2940	8.5564	8.8818	9.2103	9.5178	10.6828	11.4468
80	8.8247	8.9872	9.2103	9.4572	9.7050	10.7451	11.4763
100	9.2496	9.3588	9.5178	9.7050	9.9035	10.8198	11.5129
200	10.6066	10.6359	10.6828	10.7451	10.8198	11.2898	11.7753
300	11.4120	11.4252	11.4468	11.4763	11.5129	11.7753	12.1007

4.3 Bound preservation of the sq-model

Suppose that we have a discrete data that is generated from a bounded phenomenon, either in a two-dimensional space or in dimension three. When we attempt to visualize the data using approximation methods, it is natural to expect the approximation to adhere to the boundedness [26, 25]. The sq-curves and sq-surfaces fulfill the convex hull property, which is the powerful feature that guarantees the bound-preserving approximation. Actually this is a feature that is in common for all Bézier-like model with convex hull property. When we approximate a data with a Bézier-like model, the curve or surface lies in the convex hull of the control points. If we set the data to be the control points, then the curve (surface) would be entirely inside the control polygon (control net), which guarantees the boundedness.

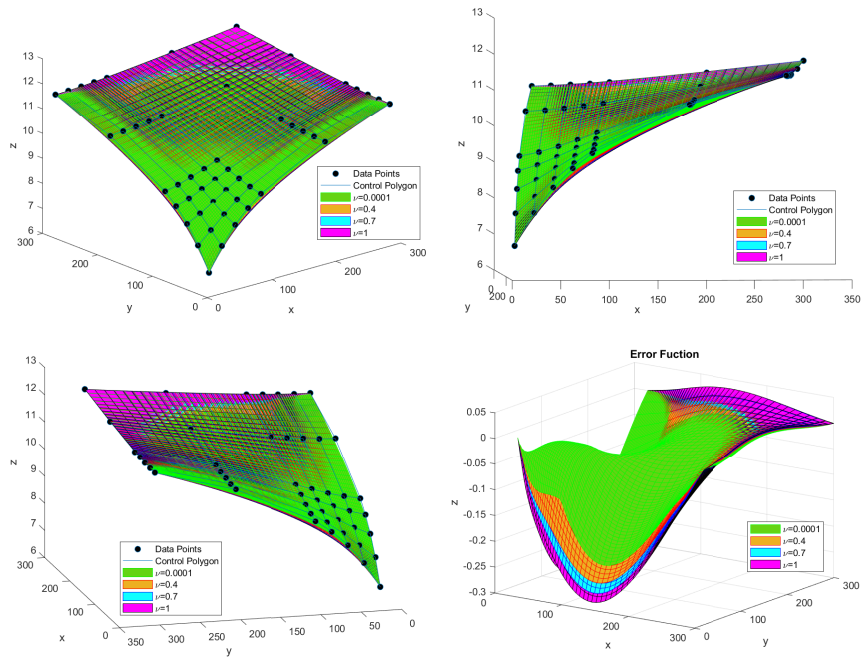


Figure 5: Axial monotonicity-preserving approximation with different shape parameters and the error functions

5 Conclusion

We presented Bézier-like parametric curves and surfaces through introducing a new class of blending functions with one shape parameter. These curves and surfaces, in addition to covering many properties of classical Bézier models, can be adjusted in a shape by altering the shape parameter when the control points are fixed. It is been verified that the newly defined sq-models can be successfully used for monotonicity-preserving approximation. The bound preservation property of the sq-models has also been reviewed.

Note that the introduction of shape parameter not only brings an advantage to the shape modification of the Bézier-like curves but also provides an optimized parameter for the shape optimization design of the Bézier-like ones. Hence, the research on how to utilize the SDABWO [12] to solve the model of curve shape optimization, which takes the shape parameter as the optimization variables, could be addressed in future works.

References

1. Abbas, M., Majid, A.A. and Ali, J.M. *Monotonicity-preserving $C2$ rational cubic spline for monotone data*, Appl. Math. Comput., 219(6) (2012), 2885–2895.
2. Abbas, M., Majid, A.A., Awang, M.H. and Ali, J.M. *Shape-preserving rational bi-cubic spline for monotone surface data*, WSEAS Trans. Math. 11(7) (2012), 660–673.
3. Abbas, M., Majid, A.A., Awang, M.N.H. and Ali, J.M. *Monotonicity-preserving rational bi-cubic spline surface interpolation*, Sci. Asia S, 40 (2014), 22–30.
4. Bashir, U., and Ali, J. M. *Rational cubic trigonometric Bézier curve with two shape parameters*, Comput. Appl. Math. 35(1) (2016), 285–300.
5. BiBi, S., Abbas, M., Misro, M.Y. and Hu, G. *A novel approach of hybrid trigonometric Bézier curve to the modeling of symmetric revolutionary curves and symmetric rotation surfaces*, IEEE Access, 7 (2019), 165779–165792.
6. BiBi, S., Abbas, M., Miura, K.T. and Misro, M.Y. *Geometric modeling of novel generalized hybrid trigonometric Bézier-like curve with shape parameters and its applications*, Mathematics, 8(6) (2020), 967.
7. Carnicer, J.M., Garcia-Esnaola, M. and Peña, J.M. *Convexity of rational curves and total positivity*, J. Comput. Appl. Math. 71(2) (1996), 365–382.
8. Chen, J. and Wang, G.J. *A new type of the generalized Bézier curves*, Appl. Math. J. Chinese Univ. Ser. B, 26(1) (2011), 47–56.

9. Farin, G. E., and Farin, G. *Curves and surfaces for CAGD: a practical guide*, Morgan Kaufmann, 2002.
10. Floater, M.S. and Peña, J.M. *Tensor-product monotonicity preservation*, Adv. Comput. Math. 9(3) (1998), 353–362.
11. Hu, G., Bo, C., Wei, G. and Qin, X. *Shape-adjustable generalized Bézier Surfaces: Construction and its geometric continuity conditions*, Appl. Math. Comput. 378 (2020), 125215.
12. Hu, G., Du, B., Wang, X. and Wei, G. *An enhanced black widow optimization algorithm for feature selection*, Knowl Based Syst. 235 (2022), 107638.
13. Hu, X., Hu, G., Abbas, M. and Misro, M.Y. *Approximate multi-degree reduction of Q -Bézier curves via generalized Bernstein polynomial functions*, Adv. Differ. Equ., 2020(1) (2020), 1–16.
14. Hu, G. and Wu, J.L. *Generalized quartic H -Bézier curves: Construction and application to developable surfaces*, Adv. Eng. Softw. 138 (2019), 102723.
15. Hu, G., Wu, J. and Qin, X. *A new approach in designing of local controlled developable H -Bézier surfaces*, Adv. Eng. Softw. 121 (2018), 26–38.
16. Hu, G., Wu, J. and Qin, X. *A novel extension of the Bézier model and its applications to surface modeling*, Adv. Eng. Softw. 125 (2018), 27–54.
17. Juhász, I. *A NURBS transition between a Bézier curve and its control polygon*, J. Comput. Appl. Math. 396 (2021), 113626.
18. Kovács, I. and Várady, T. *P -curves and surfaces: Parametric design with global fullness control*, Computer-Aided Design, 90 (2017), 113–122.
19. Kovács, I. and Várady, T. *P -Bézier and P -Bspline curves—new representations with proximity control*, Computer Aided Geom. Des. 62 (2018), 117–132.
20. Li, J. *A novel Bézier curve with a shape parameter of the same degree*, Results Math. 73(4) (2018), 1–11.
21. Majeed, A., Abbas, M., Qayyum, F., Miura, K.T., Misro, M.Y. and Nazir, T. *Geometric modeling using new Cubic trigonometric B -Spline functions with shape parameter*, Mathematics, 8(12) (2020), 2102.
22. Maqsood, S., Abbas, M., Hu, G., Ramli, A.L.A. and Miura, K.T. *A novel generalization of trigonometric Bézier curve and surface with shape parameters and its applications*, Math. Probl. Eng. 2020, Art. ID 4036434, 25 pp.

23. Maqsood, S., Abbas, M., Miura, K.T., Majeed, A. and Iqbal, A. *Geometric modeling and applications of generalized blended trigonometric Bézier curves with shape parameters*, Adv. Differ. Equ. 2020(1) (2020), 1–18.
24. Qin, X., Hu, G., Zhang, N., Shen, X. and Yang, Y. *A novel extension to the polynomial basis functions describing Bézier curves and surfaces of degree n with multiple shape parameters*, Appl. Math. Comput. 223 (2013), 1–16.
25. Saeidian, J., Sarfraz, M., Azizi, A. and Jalilian, S. *A new approach of constrained interpolation based on cubic Hermite splines*, J. Math. 2021, Art. ID 5925163, 10 pp.
26. Saeidian, J., Sarfraz, M. and Jalilian, S. *Bound-preserving interpolation using quadratic splines*, Journal of Mathematical Modeling, (2020), 1–13.
27. Sarfraz, M., Hussain, M.Z. and Hussain, F. *Shape preserving convex data interpolation*, Appl. Comput. Math. 16(3) (2017), 205–227.
28. Sarfraz, M., Samreen, S. and Hussain, M.Z. *A Quadratic Trigonometric Nu Spline with Shape Control*, Int. J. Image Graph. 17(03) (2017), 1750015.
29. Tariq, Z., Ibraheem, F., Hussain, M.Z. and Sarfraz, M. *Monotone data modeling using rational functions*, Turk. J. Electr. Eng. Comput. Sci. 27(3) (2019), 2331–2343.
30. Usman, M., Abbas, M., and Miura, K.T. *Some engineering applications of new trigonometric cubic Bézier-like curves to free-form complex curve modeling*, J. Adv. Mech. Des. Syst. Manuf. 14(4) (2020), JAMDSM0048-JAMDSM0048.
31. Yan, L. *Adjustable Bézier curves with simple geometric continuity conditions*, Math. Comput. Appl. 21(4) (2016), 44.
32. Yan, L. and Liang, J. *An extension of the Bézier model*, Appl. Math. Comput. 218(6) (2011), 2863–2879.

How to cite this article

B. Nouri and J. Saeidian On a class of Bézier-like model for shape-preserving approximation. *Iranian Journal of Numerical Analysis and Optimization*, 2022; 12(2): 449-466. doi: 10.22067/ijnao.2022.72818.1064.